Korean J. Chem. Eng., 33(3), 880-884 (2016)
DOI: 10.1007/s11814-015-0200-1

pISSN: 0256-1115
eISSN: 1975-7220

Semi-transparent thin film solar cells by a solution process

Van Ben Chu[*,], Se Jin Park[*], Gi Soon Park[*], Hyo Sang Jeon[*], Yun Jeong Hwang[*,**], and Byoung Koun Min[*,**,***,†]**

*Clean Energy Research Center, Korea Institute of Science and Technology, 39-1, Hawolgok-dong, Seongbuk-gu, Seoul 02792, Korea
**Korea University of Science and Technology, 176, Gajeong-dong, 217, Gajeong-ro, Yuseong-gu, Daejeon 34132, Korea
***Green School, Korea University, Anam-dong, Seongbuk-gu, Seoul 02841, Korea
(*Received 26 May 2015 • accepted 19 September 2015*)

Abstract−Easily processed, low cost, and highly efficient solar cells are desirable for photovoltaic conversion of solar energy to electricity. We present the fabrication of precursor solution processed $CuInGaS_2$ (CIGS) thin film solar cells on transparent indium tin oxide (ITO) substrates. The CIGS absorber film was prepared by a spin-coating method, followed by two successive heat treatment processes. The first annealing process was on a hot plate at 300 °C for 30 min in air to remove carbon impurities in the film; this was followed by a sulfurization process at 500 °C in an H_2S(1%)/Ar environment to form a polycrystalline CIGS film. The absorber film with an optical band-gap of 1.52 eV and a thickness of about 1.1 μm was successfully synthesized. Because of the usage of a transparent glass substrate, a bifacial CIGS thin film device could be achieved; its power conversion efficiency was measured to be 6.64% and 0.96% for front and rear illumination, respectively, under standard irradiation conditions.

Keywords: Solar Cell, CIGS, ITO, Precursor Solution, Thin Film

INTRODUCTION

Photovoltaics (PV), which directly convert photon energy to electrical energy, have become an important part of renewable energy programs because of the unlimited nature of solar energy. PV systems are now not only harvesting energy on rooftops, but are being integrated into building blocks for multiple functions, such as harvesting energy, power generating windows, building ceilings, and intelligent light [1,2]. Particularly for window applications, some portion of the sunlight should be transmitted through the building's integrated PV system. This can be achieved by employing a wide band-gap absorber material and a transparent substrate in the solar cell devices.

Among wide band-gap semiconductor materials, copper indium gallium disulfide ($CuIn_xGa_{1-x}S_2$) has attracted considerable attention because of its direct and adjustable band-gap with a high absorption coefficient. The band-gap of $CuIn_xGa_{1-x}S_2$ films can range from 1.46 eV (x=1) to 2.4 eV (x=0) [3] depending on the amount of Ga in the CIGS composition. Also, CIGS with a band-gap of 1.5 eV has an efficiency close to the theoretical maximum for a single junction solar cell [4]. More importantly, high band-gap solar cells can produce higher voltage, which is desirable in solar cell modules to reduce energy loss from series resistances [5].

In general, CIGS thin film solar cells have a typical device configuration of ZnO : Al/i-ZnO/CdS/CIGS/Mo-coated soda-lime glass. In this architecture, sunlight cannot be transmitted through the solar cell device because the opaque Mo layer blocks light transmission, resulting in limited applications to smart windows [6] or power generating windows [7]. To achieve light transmission, alternative substrates with good transparency such as indium tin oxide (ITO) or fluorine-doped tin oxide (FTO) have been used for CIGS solar cells. For example, Nakada et al. fabricated CIGS films on ITO and FTO by a co-evaporation method and obtained solar cell efficiencies of 15.2% and 13.7%, respectively [8]. Nishiwaki et al. also fabricated $CuGaSe_2$ (CGS) films by co-evaporation on transparent ITO substrates for the top cell of tandem solar cells and obtained a power conversion efficiency (PCE) of 4.3% [9].

To fabricate CIGS thin film solar cells on transparent glass substrates more cost-effectively, non-vacuum processes such as printing, spraying, blade coating, and spin-coating [10-13] will be required. Solution-processed CIGS thin film solar cells have been intensively developed, but most studies have used Mo-coated glass substrates. Only a few studies of solution-processed CIGS thin film solar cells on transparent glass substrate have been conducted to date [7,14].

In this study, we investigated the fabrication of conventionally structured CIGS thin film solar cells on ITO substrates by a precursor alcohol solution process. The CIGS film was deposited on commercial ITO substrates by a simple spin-coating method. A polycrystalline CIGS thin film with minimal carbon impurities and a thickness of about 1.1 μm was obtained after two heat treatment processes. A solar cell device structure (Al,Ni/AZO/i-ZnO/CdS/CIGS/ITO/Glass) was fabricated and tested, showing a power conversion efficiency of 6.64% with front illumination on an active area of 0.44 cm^2. We also tested the solar cell performance with rear side and bifacial illumination, achieving power conversion efficiencies of 0.96 and 7.6%, respectively. Notably, this solar cell efficiency is one of the highest values ever obtained for solution-processed CIGS thin film solar cells with transparent conducting glass substrates.

†To whom correspondence should be addressed.
E-mail: bkmin@kist.re.kr

EXPERIMENTAL

1. Preparation of the Precursor Solution

The precursor solutions were prepared by dissolving $Cu(NO_3)_2 \cdot xH_2O$ (99.999%, Alfa Aesar), $In(NO_3)_3 \cdot xH_2O$ (99.99%, Alfa Aesar) and $Ga(NO_3)_3 \cdot xH_2O$ (99.999%, Alfa Aesar) in methanol and then mixing with a Polyvinyl acetate (PVA, Sigma-Aldrich) binder solution. First, 927 mg $Cu(NO_3)_2 \cdot xH_2O$, 1148 mg $In(NO_3)_3 \cdot xH_2O$ and 493 mg $Ga(NO_3)_3 \cdot xH_2O$ were dissolved in 7 mL of methanol and stirred at 600 rpm for about 2 h. The binder solution was made by dissolving 1,000 mg of PVA in 7 mL of methanol and stirring at 600 rpm for 2 h. Finally, the two solutions were mixed together and stirred again until the mixture become homogeneous with a bluish color. The solution was then filtered using a 0.2 μm syringe filter.

2. Solar Cell Device Fabrication

A solar cell device with the configuration (Al,Ni/AZO/i-ZnO/CdS/CIGS/ITO/glass) was fabricated on a commercial ITO/Glass substrate (Samsung Corning, ~8 Ω/sq). Fig. 1 shows the schematic of the CIGS fabrication process using the precursor solutions. First, the precursors were dissolved and mixed with the PVA binder in methanol. Then the solution was spin-coated (2,000 rpm, 40 s) on the ITO substrate to make a precursor film. Next, the film was annealed in air on a hot plate at 300 °C for 30 min. The spin-coating and annealing processes were repeated several times to reach a desirable thickness of the CIGS film. The subsequent annealing processes in an H_2S(1%)/Ar environment for 30 min resulted in a polycrystalline CIGS film with a film thickness of ~1.1±0.1 mm. The CIGS film was etched in a diluted KCN solution to remove Cu-rich phases on the surface prior to the deposition of the buffer layer. The n-type CdS buffer layer was deposited by chemical bath deposition followed by the deposition of intrinsic and Al-doped zinc oxide window layers.

3. Characterization

The CIGS film structure was characterized by scanning electron microscopy (SEM, FEI, Nova-Nano200) with 10 kV acceleration voltage and by an X-ray diffractometer (XRD, Shimadzu, XRD-6000) with Cu-Kα radiation (λ=0.15406 nm). The thickness of the CIGS film was measured by a surface profiler (Veeco, Dektak 8). The optical properties of the CIGS absorption film and the completed solar cell device were measured with a UV-Vis spectrometer (Varian, Cary 5000). The composition of the CIGS film was investigated with an electron probe microanalyzer (EPMA, JEOL Ltd., Tokyo, Japan). The EPMA was operated at 15 kV and 20 nA current with 1 to 30 μm e-beam diameter providing a quantitative analysis of the element distribution within the CIGS film. Device performances were characterized using a solar simulator (ABET Technologies, Inc., Sun 2000) and an incident photon-to-current conversion efficiency (IPCE) measurement system (K3100, McScience).

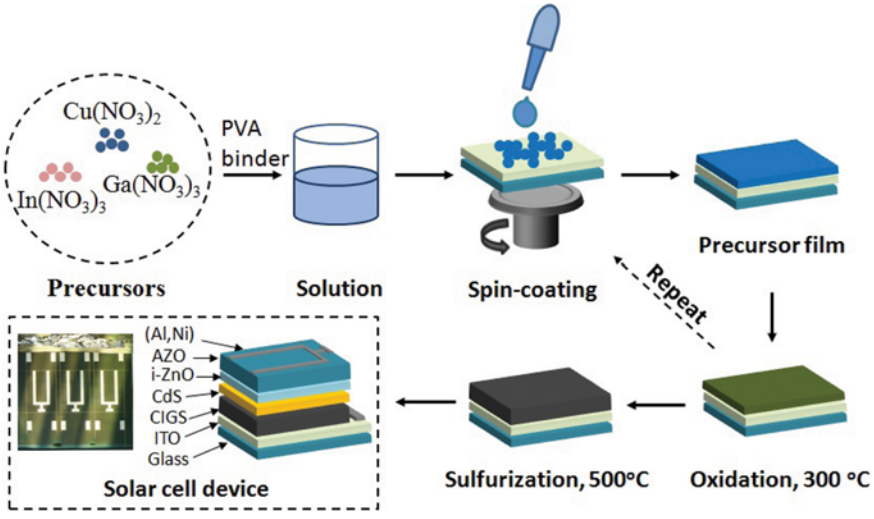

Fig. 1. Schematic of the fabrication process for the $CuInGaS_2$/indium tin oxide (CIGS/ITO) thin film solar cell using precursor solutions.

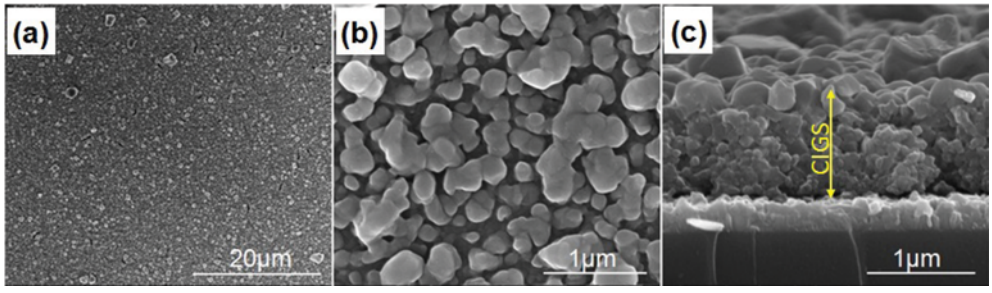

Fig. 2. Scanning electron microscope (SEM) images of CIGS absorber film growth on an ITO substrate showing the surface morphology at low magnification (2a), high magnification (2b), and a cross-sectional view (2c).

RESULTS AND DISCUSSION

The prepared precursor solution was spin-coated on an ITO substrate followed by annealing at 300 °C to remove the carbon impurities from the organic chemicals (e.g., polymer binder). An amorphous mixed-oxide film was formed after several cycles of spin-coating and annealing processes. To convert the mixed-oxide film of Cu, In, and Ga into a CIGS alloy, the film was sulfurized at 500 °C in an H_2S(1%)/Ar gas environment. Following the sulfurization process, a dark colored CIGS film remained on the ITO substrate. Fig. 2 shows the top-view and cross-sectional SEM images of the prepared CIGS films. The low magnification SEM image (Fig. 2(a)) shows a uniform surface with an absence of apparent cracks. A rough surface with larger grains on top can be also observed in the high magnification top-view (Fig. 2(b)) and the cross-sectional SEM image (Fig. 2(c)). This non-uniform morphology of the film may be attributed to small variation in chemical composition across the film.

To elucidate the composition distribution on the surface and throughout the film thickness, elemental analysis and mapping of Cu, In, Ga and S was performed out by an electron probe microanalyzer (EPMA). The average atomic composition ratios of Cu, In, Ga and S were estimated as 1 : 0.74 : 0.21 : 2.04. Fig. 3 shows the element map corresponding to the SEM image (Fig. 3(a)). A gradient distribution of Ga with a higher concentration at the bottom part of the CIGS film was observed (Fig. 3(b)). The lower amount of Ga on the surface and the higher amount at the bottom also resulted in morphology variation: the CIGS film contained larger grains in the upper part and smaller grains at the bottom [15]. The self-Ga-grading with higher Ga concentration at the bottom (close to the CIGS/ITO interface) may help to transport minority carriers to the p-n junction, hence improving the collection of charge carriers.

To absorb as much sunlight as possible, the film should have the greatest possible thickness. From the standpoint of charge carrier recombination, however, a thicker film can trigger more recombination because of the nature of the defects in solution-processed CIGS thin films, such as a high degree of grain boundaries, and impurities. Thus, optimized film thickness was assumed to be 1.1 mm in our CIGS films.

The crystal structure of the CIGS film was also investigated by X-ray diffraction (XRD). The XRD data from the CIGS/ITO films show a main peak at 27.9°, which is 2θ for the (112) plane; other apparent peaks at 2θ angles of 32.5°, 46.8° and 55.3° correspond to the (004)/(200), (220)/(204) and (116)/(312) phases, respectively (Fig. 4). The presence of an intense peak at 27.9° together with the other dominant peaks indicates the polycrystalline chalcopyrite structure of the CIGS film, which is in good agreement with the Joint

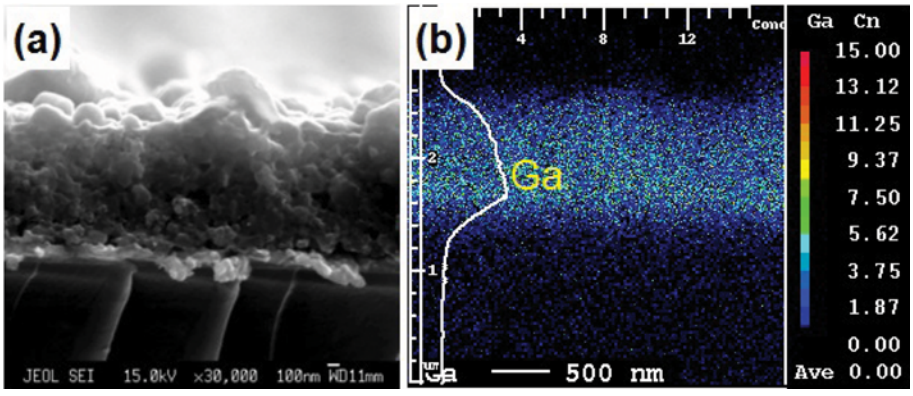

Fig. 3. Electron probe microanalyzer (EPMA) compositional mapping of the CIGS film. SEM image of mapping area (3a), EPMA mapping images of Ga (3b) with enclosed line profiles at the cross section of the CIGS/ITO film.

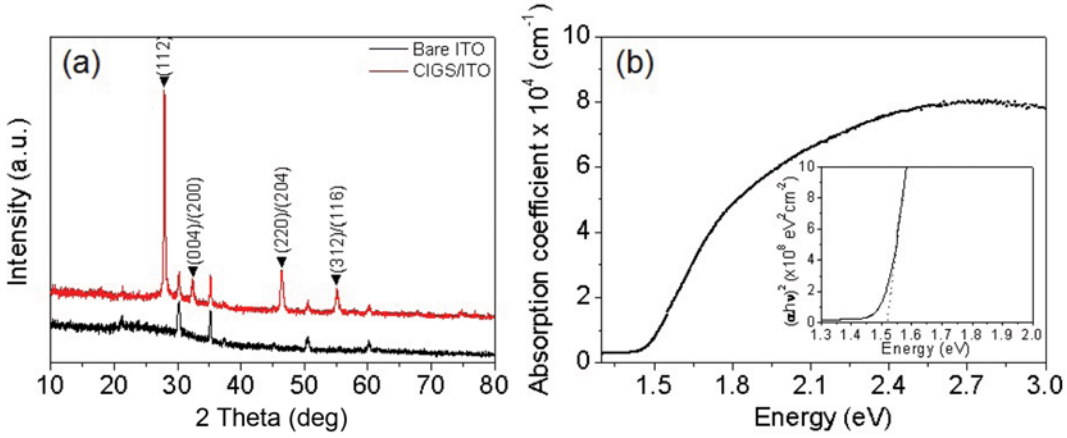

Fig. 4. X-ray diffraction (XRD) patterns of the bare ITO substrate and the CIGS/ITO films (4a) and optical properties of CIGS film (4b).

Committee on Powder Diffraction Standards reference JCPDS #27-0159. Other peaks at 2θ angles of 21.3°, 30.2°, 50.6°, and 60.3° were ascribed to ITO (JCPDS #6-416).

The optical properties of the CIGS film grown on an ITO glass substrate were also characterized by UV-Vis spectroscopy (Fig. 4(b)). CIGS is direct band-gap semiconductor; thus, the absorption coefficient of the CIGS film can be estimated from the reflectance, transmittance and thickness of the CIGS film based on the equation, $\alpha = \ln((1-R)^2/T)/d$, [16] where R, T and d indicate reflectance, transmittance and film thickness, respectively. The band-gap can also be calculated by a plot of $(\alpha h\nu)^2$ vs. photon energy ($h\nu$), which yields a value of 1.52 eV (inset of Fig. 4(b)).

The CIGS solar cell device fabricated on a transparent conductive glass substrate has a bifacial configuration where light can enter from both sides simultaneously. The device fabrication was based on well-known conventional constituents, arranged in the conventional configuration of (Al,Ni/Al : ZnO/ZnO/CdS/CIGS/ITO/Glass). The CdS (50 nm) was deposited by chemical bath deposition; the intrinsic ZnO (50 nm), and the Al : ZnO (500 nm) layers, by radio frequency magnetron sputtering methods. Fig. 5 shows the performance of the best solar cell device with front illumination (rectangles-black line) and rear illumination (circles-red line). The I-V characteristic with front illumination shows a power conversion efficiency (PCE) of 6.64% with an open circuit voltage, current density, and fill factor of 668.30 mV, 17.57 mA/cm^2, and 56.55%, respectively. The rear illumination shows a PCE of 0.96% with an open circuit voltage, current density and fill factor of 578.60 mV, 2.54 mA/cm^2 and 65.14%, respectively (Table 1). Notably, the J_{sc} value of 17.57 mA/cm^2 is similar to the best results from CIGS thin film solar cells fabricated by the sputtering method onto Mo substrates [17,18].

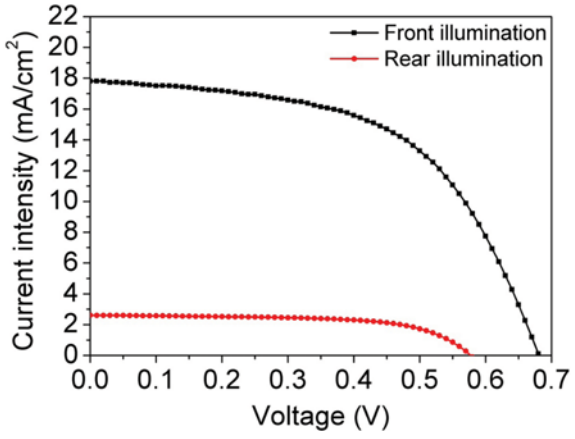

Fig. 5. I-V characteristics of the Al,Ni/AZO/i-ZnO/CdS/CIGS/ITO/Glass solar cell with front and rear illumination.

Table 1. Performance of the solar cell device with front and rear illumination

Illumination side	V_{oc} (mV)	J_{sc} (mA/cm^2)	FF. (%)	Area (cm^2)	Eff. (%)
Front	668.3	17.57	56.55	0.44	6.64
Rear	578.6	2.54	65.14	0.44	0.96

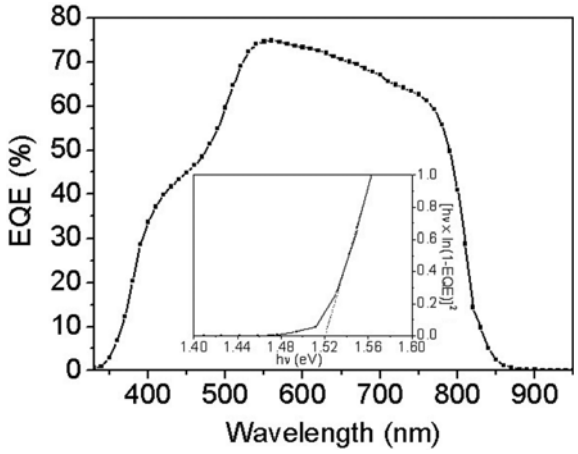

Fig. 6. External quantum efficiency (EQE) spectrum of the solar cell device. The inset provides an estimate of the band-gap of the CIGS absorber film.

The external quantum efficiency (EQE) spectrum of the CIGS/ITO solar cell device is shown in Fig. 6. The relatively high EQE of ~75% was obtained for the precursor solution processed CIGS/ITO solar cell at ~550 nm. The EQE cutoff at wavelength of ~850 nm indicates approximately the optical band-gap of the CIGS absorber. The band-gap (1.52 eV) could be estimated from the EQE data as shown in the inset of Fig. 6 in good agreement with the value obtained from the absorption data.

There is still much room for improvement in the performance of these solar cell devices. For example, doping the CIGS film with Na and K is a promising way to improve the electronic and CIGS/CdS heterojunction quality that has been demonstrated by co-evaporation methods on a flexible polyimide substrate, and showed a solar cell efficiency of 20.4% [19]. Uneven composition distribution throughout the absorber film such as double Ga grading would also improve the performance of solar cell devices [20,21]. In addition, we expect that integrating nanostructures in solar cells (e.g., nanostructured electrodes [22]) with optimized thickness would also further enhance the performance of solar cell devices; these are currently under investigation.

CONCLUSION

We have demonstrated the fabrication of a CIGS thin film solar cell, processed from a precursor solution, on a transparent ITO substrate. The CIGS film was deposited by a spin-coating process followed by two heat treatment processes: oxidation and sulfurization. The thickness of the CIGS film was about 1.1 μm with a rough surface morphology. The EPMA mapping indicated a gradient of Ga composition, with the highest concentration at the bottom of CIGS film. The solar cell device with bifacial properties showed a conversion efficiency of 6.64% for the front illumination and 0.96% for the rear illumination.

ACKNOWLEDGEMENTS

This work was supported by the Energy Technology Develop-

ment Program of the Korea Institute of Energy Technology Evaluation and Planning (KETEP) grant (No.20143030011530) funded by the Korean government. Also, the authors would like to thank the internal program of the Korea Institute of Science and Technology (KIST).

REFERENCES

1. B. P. Jelle and Ch. Breivik, *Energy Procedia*, **20**, 68 (2012).
2. R. Baetens, B. P. Jelle and A. Gustavsen, *Sol. Energ. Mater. Sol. Cells*, **94**, 87 (2010).
3. J. A. Hollingsworth, K. K. Banger, M. H. C. Jin, J. D. Harris, J. E. Cowen, E. W. Bohannan, J. A. Switzer, W. E. Buhro and A. F. Hepp, *Thin Solid Films*, **431-432**, 63 (2003).
4. M. Green, SOLAR CELLS: Operating Principles, Technology and System Applications, Prentice-Hall New Jersey, USA (1982).
5. S. Siebentritt, *Thin Solid Films*, **403-404**, 1 (2002).
6. H. K. Kwon, K. T. Lee, K. Hur, S. H. Moon, M. M. Quasim, T. D. Wilkinson, J. Y. Han, H. D. Ko, I. K. Han, B. Park, B. K. Min, B. K. Ju, S. M. Morris, R. H. Friend and D. H. Ko, *Adv. Energy Mater.*, **5**, 1401347 (2015).
7. S. H. Moon, S. J. Park, Y. J. Hwang, D. K. Lee, Y. Cho, D. W. Kim and B. K. Min, *Sci. Rep.*, **4**, 4408 (2014).
8. T. Nakada, Y. Hirabayashi, T. Tokado, D. Ohmori and T. Mise, *Sol. Energy*, **77**, 739 (2004).
9. S. Nishiwaki, S. Siebentritt, P. Walk and M. Ch. Lux-Steiner, *Prog. Photovolt: Res. Appl.*, **11**, 243 (2003).
10. W. Wang, Y. W. Su and C. H. Chang, *Sol. Energ. Mater. Sol. Cells*, **95**, 2616 (2011).
11. D. Y. Lee, S. J. Park and J. H. Kim, *Curr. Appl. Phys.*, **11**, S88 (2011).
12. M. G. Park, S. J. Ahn, J. H. Yun, J. H. Gwak, A. Cho, S. K. Ahn, K. S. Shin, D. H. Nam, H. S. Cheong and K. H. Yoon, *J. Alloys Compd.*, **513**, 68 (2012).
13. A. Cho, S. J. Ahn, J. H. Yun, J. H. Gwak, S. K. Ahn, K. S. Shin, H. J. Song and K. H. Yoon, *Sol. Energ. Mater. Sol. Cells*, **109**, 17 (2013).
14. L. Li, N. Coates and D. Moses, *J. Am. Chem. Soc.*, **132**, 22 (2010).
15. S. J. Park, J. W. Cho, J. K. Lee, K. Shin, J. H. Kim and B. K. Min, *Prog. Photovolt: Res. Appl.*, **22**, 122 (2014).
16. J. Tauc, *Amorphous and Liquid Semiconductors*, Plenum Press, New York (1974).
17. S. Merdes, D. A. Ras, R. Mainz, R. Klenk, M. Ch. L. Steiner, A. Meeder, H. W. Schock and J. Klaer, *Prog. Photovolt: Res. Appl.*, **21**, 88 (2013).
18. R. Kaigawa, A. Neisser, R. Klenk and M. Ch. L. Steiner, *Thin Solid Films*, **415**, 266 (2002).
19. A. Chirila, P. Reinhard, F. Pianezzi, P. Bloesch, A. R. Uhl, C. Fella, L. Kranz, D. Keller, Ch. Gretener, H. Hagendorfer, D. Jaeger, R. Erni, S. Nishiwaki, S. Buecheler and A. N. Tiwari, *Nat. Mater.*, **12**, 1107 (2013).
20. M. Gloeckler and J. R. Sites, *J. Phys. Chem. Solids*, **66**, 1891 (2005).
21. C. Frisk, C. P. Björkman, J. Olsson, P. Szaniawski, J. T. Wätjen, V. Fjällström, P. Salomé and M. Edoff, *J. Phys. D: Appl. Phys.*, **47**, 485104 (2014).
22. V. B. Chu, J. W. Cho, S. J. Park, Y. J. Hwang, H. K. Park, Y. R. Do and B. K. Min, *Nanotechnology*, **25**, 125401 (2014).